

DYNAMICS OF FLAME-BALL FORMATION FROM LOCALIZED IGNITION: EFFECTS OF ELEVATED PRESSURE AND TEMPERATURE

JIAO YUAN,¹ STEPHEN D. TSE² AND C. K. LAW¹

¹*Department of Mechanical and Aerospace Engineering
Princeton University
Princeton, NJ 08544, USA*

²*Department of Mechanical and Aerospace Engineering
Rutgers University
Piscataway, NJ 08854, USA*

A computational study was conducted on expanding spherical premixed flames to investigate the dynamics of flame-ball formation at elevated temperatures and pressures. Lean H₂/air mixtures were investigated using a time-dependent, spherically symmetric code with detailed chemistry, transport, and radiation submodels. Results show that, with increasing pressure, both the steady-state flame-ball radius and the H₂ consumption rate for a given mixture composition decrease monotonically up to 50 atm, varying approximately as $p^{-0.57}$. Furthermore, a window of pulsating flame behavior, near the upper dynamic flame-ball limit, was discovered and investigated. Within this window, an outwardly propagating flame begins to self-extinguish due to radiative losses but revives suddenly due to low-Lewis-number effects and evolves into a flame ball. More than one such cycle of behavior can occur for a given mixture concentration. Results further show that as the ambient mixture temperature is increased, the initial trend is a downward shift of the upper dynamic flame-ball limit. With reduced radiative loss, spherical flames continue to propagate outwardly for leaner mixture compositions without degenerating into flame balls, but at the same time, expand themselves into radiative extinction. Again, the role of radiative loss as both the requisite mechanism for and the limiting mechanism against the dynamic transformation of spherically propagating flames into flame balls is emphasized. Nonetheless, as the ambient temperature is increased to near 700 K (in an attempt to investigate the boundary defining the flameless combustion regime), steady flame balls are no longer attainable, with chemical reactions occurring at the boundary.

Introduction

Recent works [1] have shown that the flame ball [2] is not a particular phenomenon isolated from the propagating flame. It was found [1] that depending on the chemical, diffusive, and radiative aspects of a subunity *Le* propagating flame initiated by an ignition kernel, the flame will either expand until self-extinction or degenerate and evolve into a stationary flame ball. Consequently, flame propagation can persist beyond the classical lean and rich flammability limits based on the propagation of the one-dimensional planar flame.

Studies on flame balls [2–6] as well as the recent extensions [1] have shown that radiative loss is inherent to the flame propagation in that it serves not only to stabilize stationary flame balls, but is also responsible for both the dynamic creation and the preclusion of flame balls from different centrally ignited premixtures [1]. For example (see Fig. 1, reproduced from Ref. [1]), for hydrogen in air at 1 atm, spherically expanding flames can degenerate and evolve into stationary flame balls for mixture compositions in the range of $3.5\% \approx X_{H_2} \approx 6.5\%$. For

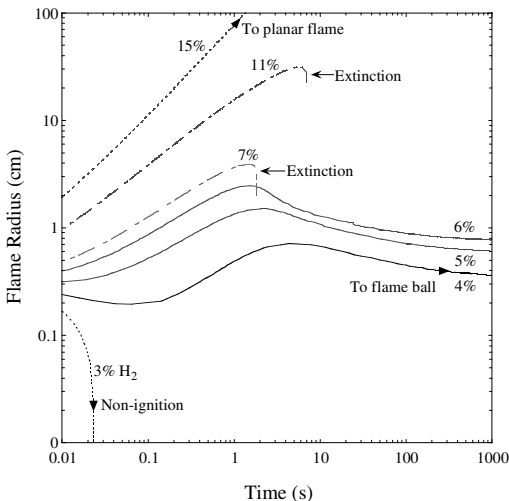


FIG. 1. Flame trajectories at STP showing possible evolutions of expanding flame to flame ball, permanent extinction, and planar flame, with increasing hydrogen concentration in air.

6.5% $\approx X_{\text{H}_2} \approx 11\%$, flames propagate until radiative extinction, never evolving into flame balls, while for $X_{\text{H}_2} \approx 11\%$, the expanding spherical flames develop asymptotically into planar flames. These results present a dynamic range of flame ball formation that is much narrower than that predicted for the statically produced steady flame balls (3.5% $\approx X_{\text{H}_2} \approx 10.7\%$) [7]. Nonetheless, despite the seemingly limited range of subsistence for the flame ball itself, its dynamics, as described above, are intimately related to the self-extinguishing flame phenomenon.

In the present investigation, we extend the work of Ref. [1] to environments of elevated pressures and temperatures. The study is motivated by both theoretical and practical considerations. With convection effects approaching zero, steady flame balls become controlled by the simplest interaction of chemical kinetic and transport processes, providing test scenarios for the extraction of fundamental parameters to enable comprehensive modeling of combustion chemistry and processes. In terms of practical interests, we note that high-pressure combustion promotes cycle efficiency in general and reduces pollutant formation through ultralean operations. Furthermore, since $Le < 1$ for lean hydrogen and methane combustion in air, the dynamics of flame balls and self-extinguishing flames come into prominence. In particular, since microscale systems easily accommodate elevated pressures, because the total containment force is small, and buoyancy forces are minimized due to the small length scales, the size, structure, and dynamics of flame balls and sublimit propagating flames can dominate the combustion characteristics. Moreover, these microscale systems can be further exploited through the recently developed technology of high-temperature air combustion where energy from exhaust gas preheat the reactants so that ultralean, super-adiabatic combustion is achieved. As the flameless combustion regime is encroached upon, profound effects on sublimit flame behavior can occur.

To explore such inherently unsteady and history-sensitive flame responses at elevated pressures and temperatures, a detailed unsteady computational simulation using realistic descriptions of chemical, diffusive, and radiative aspects of the system has been conducted. Moreover, since the phenomena here are basically consequences of the relative magnitudes of heat generation and radiative loss, we have used the hydrogen concentration in subunity Le (since flame balls can be observed only for $Le < 1$ [8]), lean hydrogen/air mixtures as the system variable to track the flame response. The problem studied is defined in the next section, which is followed by presentation and discussion of the results.

Problem Definition

The simulation employs the one-dimensional, time-dependent flame code of Rogg [9], with detailed chemical, transport, and optically thin radiation models. Other works [7,10] have examined quite extensively the effect of different chemical kinetic models on steady flame balls. Since chemistry is not the main focus of the present work, only a single detailed kinetic mechanism [11], involving nine species and 21 elementary reactions, is applied here.

Using the small-Mach-number approximation, where the thermodynamic pressure is constant throughout the flow field, the governing equations in Lagrangian coordinates for spherically symmetric flow, based on the mass-weighted coordinate,

$$\psi(r, t) = \int_0^r \rho(r, t) r^2 dr$$

are

$$c_p \rho \frac{\partial T}{\partial t} = \rho \frac{\partial}{\partial \psi} \left(\rho r^4 \lambda \frac{\partial T}{\partial \psi} \right) - \sum_{i=1}^N h_i \omega_i - \rho r^2 \frac{\partial T}{\partial \psi} \sum_{i=1}^N c_p j_i - q_{\text{rad}} + q_e \quad (1a)$$

$$\frac{\partial \rho}{\partial t} = -\rho^2 \frac{\partial(r^2 u)}{\partial \psi}, \quad \rho \frac{\partial Y_i}{\partial t} = -\rho \frac{\partial(r^2 j_i)}{\partial \psi} + \omega_i, \quad p = \frac{\rho RT}{M} \quad (1b-1d)$$

where t is the time, r is the radius, u is the radial velocity, ρ is the density, T is the temperature, p is the pressure, c_p and λ are the constant-pressure heat capacity and thermal conductivity of the mixture, respectively, R is the universal gas constant, M is the mass averaged molecular weight of the mixture, and N is the total number of species. Furthermore, Y_i , ω_i , h_i , and j_i are the mass fraction, the mass rate of production, the specific enthalpy, and the mass diffusion flux of the i th species, respectively.

For optically thin radiation,

$$q_{\text{rad}} = 4\alpha_p \sigma (T^4 - T_\infty^4) \quad (2)$$

where σ is the Stefan-Boltzmann constant and α_p is the total Planck mean absorption coefficient. Radiation heat loss is considered to be emitted only from H_2O . Planck mean absorption/emission coefficients based on a wide-band model are taken from Hubbard and Tien [12].

Ignition is achieved by energy deposition centered at zero radius, such that

$$q_e = \frac{\Delta}{\tau_s} \exp\left[-\left(\frac{r}{r_s}\right)^8\right] \text{ for } t \leq \tau_s, \quad \text{and } q_e = 0 \text{ for } t > \tau_s \quad (3)$$

where Δ is the density, r_s is the radius, and τ_s is the

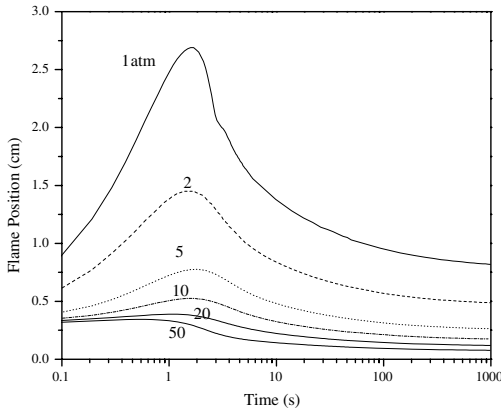


FIG. 2. Dependence of the dynamic flame ball formation process (and final size) on pressure, for 6% H_2 in air at 300 K.

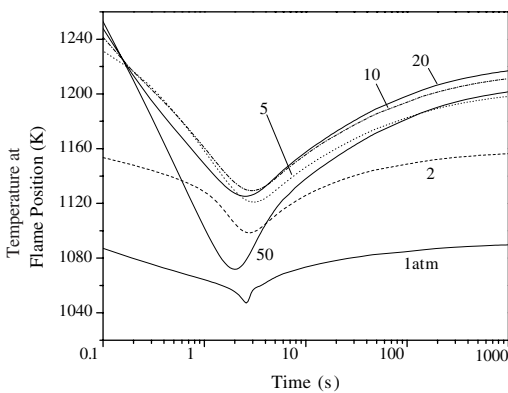


FIG. 3. Variations of the flame temperature during the flame ball formation process (corresponding to Fig. 2), for different pressures, for 6% H_2 in air at 300 K.

duration of the source energy. A typical ignition energy is $30 \times p$ [atm] mJ, which is comparable to those used in earlier simulations and experimentation at 1 atm. Different localized ignition kernels of reasonable temporal and spatial sizes were tested, and as found in Ref. [1], the flame responses are independent of the ignition source after a rapid transient period. It is conceivable that large ignition kernels can affect flame ball formation for mixture compositions bordering the self-extinguishing flame regime, to be discussed in detail later, pushing them into that regime. Otherwise, the results confirm that the phenomenon is controlled by the dynamics of the flame front instead of the ignition energy.

At $r = 0$, zero-gradient conditions are enforced. At the ambience side, boundary conditions imposed are temperature, T_∞ , fixed mixture composition, and radiative emissivity of unity. An outer boundary radius of 1 m is used. System pressures range from 1

to 50 atm, and ambient temperatures range from 300 to 700 K. Verification tests, with fixed grid points and smaller time steps, showed that the results obtained, including those for the pulsating flames, were independent of the autogrid schemes in the code and the time step used.

Results and Discussion

Pressure Effects and Flammability Boundaries

For simplicity in presenting the role of radiative heat loss on the dynamics of flame-ball formation, the results given in this section are based on calculations employing optically thin radiation with the Planck mean absorption/emission coefficients of Hubbard and Tien [12]. With respect to the scope of this work, the effects of reabsorption have been found to be mainly quantitative (e.g., limited calculations revealed that reabsorption can shift the transition boundaries) and do not affect the discussion of the underlying physical mechanisms. Radiative reabsorption mapping calculations are computationally intensive and are the subject of future work.

The flame radius, defined as the location of peak heat release rate, is plotted in Fig. 2 as a function of time for different pressures at a fixed concentration of 6% H_2 in air at 300 K. The corresponding temperature at the flame position is shown in Fig. 3. It is seen that, with increasing pressure, the entire trajectory of the flame, as well as the resultant steady-state flame-ball radius, are reduced. The turning point in the flame trajectory is the transition state at which radiative loss has sufficiently slowed down the flame and modified its structure from that of a thin propagating flame to that of a diffusion-broadened flame ball. The flame temperature immediately after the turning point however is still high, as shown in Fig. 3, and the reaction continues at a significant rate. Since radiative loss per unit volume is proportional to the pressure in the optically thin approximation, flames at higher pressures suffer more radiative loss and hence reach the turning points at smaller radii, as shown. The inset of Fig. 4 shows the evolution of the propagating flames into flame balls and affirms that the resulting peak heat release rates of the final flame balls increase with the pressure.

Figure 4 shows that the steady-state flame-ball radius and the total H_2 consumption rate for a given mixture composition scales approximately as $p^{-0.57}$, with total H_2 consumption and total heat-release rate decreasing with pressure. This result is reasonable because total radiative loss, with the optically thin approximation, scales roughly as $r_f^3 p$. Furthermore, since ρD is constant with pressure, the total heat-generation rate should scale as $r_f^2 (dY/dr)_{r_f} \sim r_f$. Therefore, with the total heat-generation rate equal to the total heat-loss rate for the steady-state flame

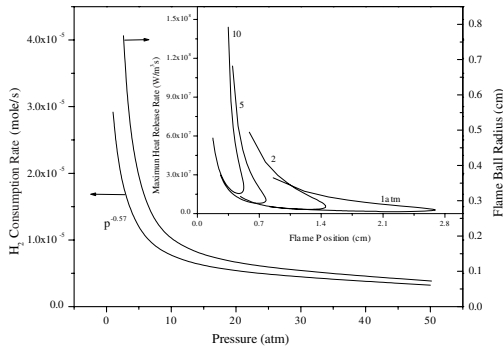


FIG. 4. Pressure effect on the final flame ball radius and the total H_2 consumption rate. The inset shows the dynamic evolution of a flame into a flame ball in the phase space of maximum heat release rate versus instantaneous flame position, for the 6% H_2 in air case at different pressures.

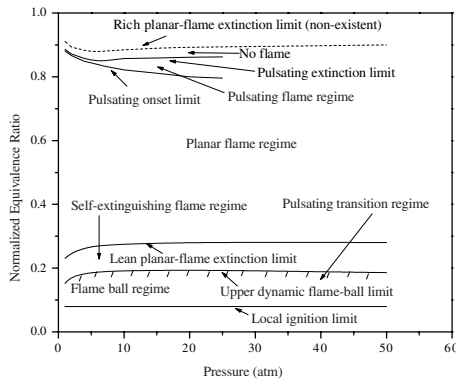


FIG. 5. Flammability map of possible flame regimes and boundaries for H_2 in air, in terms of normalized equivalence ratio ($\phi/(1 + \phi)$) and pressure.

ball, the final flame-ball radius would scale as $p^{-0.5}$, which is the dependence experimentally found in Ref. [13] for 0.5 to 2.5 atm, and is close to the present correlation. A different and more accurate power dependence law could result by considering radiative reabsorption of gases.

To discuss and appreciate the full spectrum of dynamic responses from centrally ignited flames, extensive calculations were performed to obtain the complete map of the various flammability boundaries for H_2 in air as a function of pressure, as shown in Fig. 5, where the normalized equivalence ratio, given by $\phi/(1 + \phi)$, is a more convenient parameter to gauge effects caused by fuel-lean to fuel-rich variations. The evolution of the flame dynamics can be discussed for a given pressure and increasing equivalence ratios. Here the bottom-most line represents a lean local ignition limit, which is found to be a weak

function of pressure. This limit is not caused by radiative loss because, even under adiabatic conditions, a self-propagating spherical flame cannot be established from a finite ignition source for hydrogen concentrations smaller than this value. As such, this local ignition limit can be identified as a lean flammability limit of the mixture for situations involving ignition kernels [1]. Above this limit, radiation-stabilized stationary flame balls are formed, where an ignited spherical flame initially propagates outwardly, but then recedes inwardly, with a negative flame speed, as it slowly evolves into a diffusion-dominated flame structure, as seen in Figs. 1 and 2. If expanding spherical flames propagate to larger flame sizes, volumetric radiative-loss rates eventually overcome chemical heat-release rates to the degree that they end in abrupt extinction, establishing the upper dynamic limit of flame-ball formation. This is therefore also the onset limit for self-extinguishing flames. With continuous increase in the fuel concentration, the outwardly propagating flames reach the state that they can evolve asymptotically into planar flames, in spite of radiative loss. This establishes the lean planar-flame extinction limit, which is also the flammability limit conceptually defined by Spalding and recently formalized by Law and Egolfopoulos [14] based on the failure of propagation of the planar flame due to radiative loss and kinetic weakening.

Beyond this lean planar-flame extinction limit, planar flames with radiative heat loss can exist into the rich regime until the flames start to become pulsatingly unstable, which is characteristic of $Le > 1$ flames which are relevant for rich hydrogen/air mixtures. Then there exists a regime of flame propagation in the pulsating mode [15], until the pulsating extinction limit is reached at which the pulsating flames would self extinguish. Flame propagation is not possible any more beyond this limit, although we have also indicated a rich planar-flame extinction limit, which is just the rich flammability limit of Spalding and of Law and Egolfopoulos.

The above discussion and Fig. 5 illustrate the richness of flame dynamics, including the various limits of extinguishment. Fig. 5 also shows the existence of a small, albeit important, pulsating transition regime bordering the lean planar-flame extinction limit, which was discovered in the present study and will be discussed in the next section. The present exposition also has not considered three-dimensional effects in terms of flame extinction and flame front cellular instability, which will further enrich the potential flame dynamics.

Pulsating Transition to Flame Ball

In the present study we have discovered a window of pulsation as a propagating flame evolves into a flame ball, shown with the narrow cross-hatches in Fig. 5. The lower boundary of this regime is left

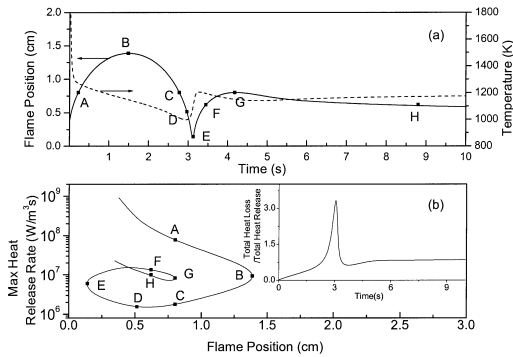


FIG. 6. Parametric representation of the pulsating evolution of an expanding flame to flame ball, for 7.3% H_2 in air at 5 atm.

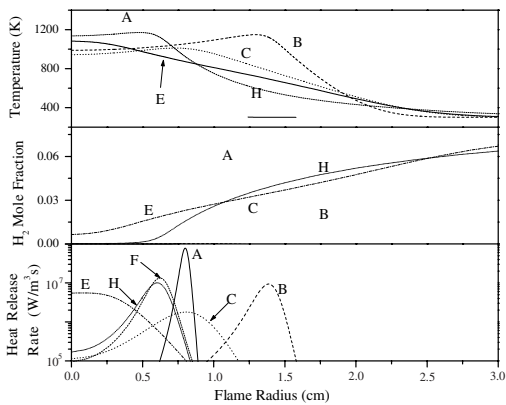


FIG. 7. Evolution of the flame structure during the pulsating transition of an expanding flame to flame ball (corresponding to Fig. 6), for 7.3% H_2 in air at 5 atm.

open as we have not succeeded in determining it precisely. Fig. 6 shows the detailed pulsating transition from propagating flame to flame ball. Here, an outwardly propagating flame is weakened due to radiative loss and reverses in direction (Fig. 6a), establishing the first turning point (A \rightarrow B \rightarrow C). The precipitous drop in flame radius (C \rightarrow D) seems to indicate imminent extinction, similar to the case in Fig. 1. However, the maximum temperature (Fig. 6a) and peak heat-release rate (Fig. 6b) begin to rise (D \rightarrow E), and then the flame reverses in direction, propagating outwardly again (E \rightarrow F). Once more, the flame is weakened due to radiative losses, but at a smaller radius and slightly smaller peak heat-release rate (Fig. 6b), and reverses in direction establishing the second peak (F \rightarrow G \rightarrow H). However, this time, as more similar to the cases in Fig. 1, the flame slowly evolves into a flame ball. Multiple pulsations have also been found to occur closer to the upper dynamic flame-ball limit.

Study of the flame structure evolution yields physical insight into this pulsating phenomenon. Fig. 7 shows elements of the flame structure (H_2 mole fraction, heat-release rate, temperature) at different points in the physical and phase trajectories of the flame of Fig. 6. For point A, the flame structure in terms of the diffusive properties of temperature and H_2 concentration is that of the conventional propagating premixed flame with a localized structure, characterized by exponential decay in the profiles. At point C, which has the same flame radius as that of point A, the flame assumes a diffusion-dominated profile and appears to be extinguishing due to radiative loss, with low heat-release rate and significant reactant leakage (see Fig. 7). However, due to the low- Le property of the mixture, the heat diffuses outward slowly, maintaining a concentrated region of high temperature near the center, while fresh H_2 reactant diffuses in quickly (see Fig. 7). With O_2 being abundant everywhere for the lean mixture, a combustible mixture eventually forms in this hot pocket and the mixture reignites (see inset of Fig. 6b), propagating outwardly again. As seen at point D, the reignition and increase in temperature occur before the flame reverses in direction and repropagates outwardly. For points F and G, where G corresponds to the second maximum flame radius, the flame structure is again similar to that of the conventional propagating premixed flame, but with a lesser localized structure than that at, say, point A. Nonetheless, by point H, which has the same flame radius as that of point F, the flame structure possesses the $1/r$ character, along with vanishing H_2 leakage, which is indicative of the flame ball. It is of interest to note that each successive peak/valley in flame position is lower/higher in magnitude. This is most likely caused by the progressive altering of the flame structure toward a more diffusive one, resulting in higher local valley magnitudes of reignition, while continued radiative loss from previously diffused products results in reduced local-peak magnitudes of turning points.

We note in passing that Buckmaster et al. [3] has predicted oscillations in the radius of flame balls, for infinitely large structures, increasing in amplitude until extinction. These oscillations are manifested only when far-field loss is dominant for Le larger than that for H_2 /air mixtures ($Le \sim 0.3$). In contrast, our pulsating flame behavior is mechanistically different, with flame structure transitioning between premixed-flame-like and diffusion-flame-like due to near-field radiative loss, decreasing in oscillation amplitude and resulting in stable flame-ball formation.

Elevated Temperature Effects

We now study the effects of elevated ambient temperatures. Fig. 8 shows the flame-ball boundaries (Fig. 5) for ambient mixture temperatures of 300

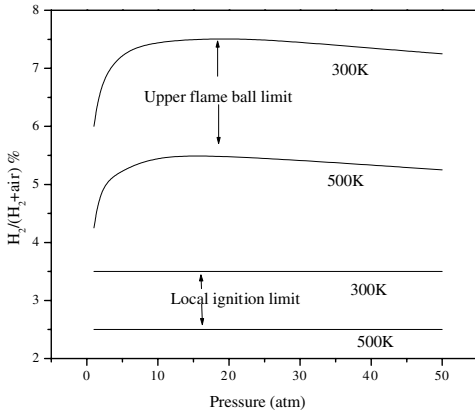


FIG. 8. Dependence of the flame-ball limits on the ambient temperature and pressure, for H_2 in air.

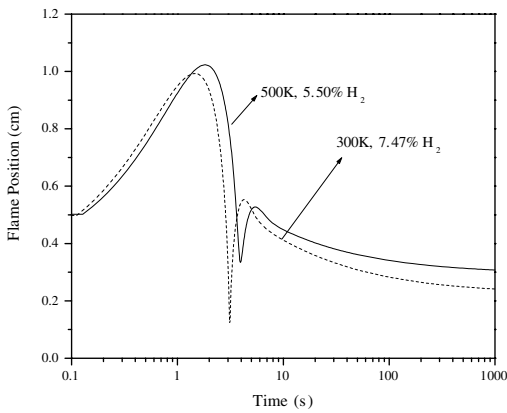


FIG. 9. Comparison of flame to flame-ball trajectories for conditions near the upper flame-ball limit of Fig. 8.

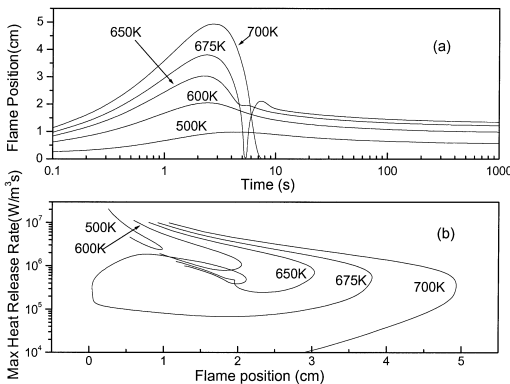


FIG. 10. Effect of elevated ambient temperature on the dynamics of flame ball formation, for 3% H_2 in air at $P = 10$ atm. Note that the 300 K case is not shown because it cannot be centrally ignited.

and 500 K. It is seen that as the ambient mixture temperature is increased, the initial trend is a downward shift of the upper dynamic flame-ball limit. With reduced radiative loss with respect to heat release, spherical flames continue to propagate outwardly for leaner mixtures without degenerating into flame balls, but at the same time, expand themselves into radiative extinction. At the corresponding upper flame-ball limit (from Fig. 8) for a given pressure (e.g., 10 atm), Fig. 9 shows that the flame trajectory for the 500 K case is only slightly larger than the 300 K case, supporting the argument that the flames extinguish due to radiation upon reaching a critical size. Additionally, with increased global enthalpy, the (adiabatic) local-ignition limit also shifts downward. It is seen that a flame ball can be dynamically formed at 3% H_2 in air at 500 K. With increasing ambient temperature, flame balls become larger in size, undergo the pulsating transition as previously described, and self-extinguish (e.g., at 700 K). The effect of increased ambient temperature is similar to the parametric increase in H_2 percentage in Fig. 1, where the flame-size response to increased flame strength (Fig. 10b) can become self-defeating due to the volumetric dependence of radiative losses.

Studies on outwardly propagating flames [16] have frequently assumed that the flame radius is much larger than the flame thickness such that both the structure and flame velocity are only slightly different from those of the planar flame. However, elevated temperatures not only affect the radiative structure of the flame but also the heat release rate. For example, at 2 atm, for 3% H_2 with 675 K ambient temperature, reactions occur even at the boundaries. The increase of reaction rates from increased pressure pushes the flame dynamics into the flameless combustion regime, establishing another manner of limiting flame-ball formation other than the self-extinction phenomenon described above.

Finally, flames at 10 atm with 4.5% H_2 were investigated to assess the dual impact of elevated temperature and pressure. The flame trajectories and the resulting flame balls are much smaller than those of Fig. 10, as expected. However, elevated ambient temperatures (~ 650 K) still extinguish the flame, based on the previous arguments.

Concluding Remarks

This work has identified various responses of centrally ignited, subunity Lewis number flames to elevated pressure and temperature variations. Results show that flame trajectories leading to flame balls are considerably smaller at elevated pressures. Elevated pressures and temperatures also extend the range of existence for a previously undetected, innate pulsating transition from propagating flame to flame ball. Previous analyses have found stationary

flame balls to be unstable to three-dimensional perturbations [17]. Gerlinger et al. [18] numerically simulated three-dimensional spherically ignited flame structures that, only with slight perturbations, exhibit growing, splitting, and extinguishing flame structures that can lead to quasi-steady flame balls. Our one-dimensional pulsating transition to flame ball could provide correlations in multidimensions and induce the flame-ball-breakup phenomenon found in experiments and computations. As a result, further investigation is needed to determine the influence of the dimensional effects on the path of flame-ball formation from ignition.

Particularly interestingly, elevated temperatures can cause flames to self-extinguish for mixtures that would otherwise form flame balls at lower ambient temperatures, even at elevated pressures. At the same time, depending on the combination of elevated temperature and pressure, flame-ball phenomena can be limited as the flameless combustion regime is encroached upon. Finally, calculations show that gas-phase radiative reabsorption only quantitatively modifies the transition boundaries for self-extinguishing flames, pulsating transition flames, and flame balls. Qualitative differences from the optically thin cases are expected to arise only for systems with highly absorptive species, such as CO_2 , in the far field.

Acknowledgment

This research was supported by NASA under its Microgravity Combustion Program and a center grant on carbon mitigation from the British Petroleum Corp. to Princeton University.

REFERENCES

1. Tse, S. D., He, L., and Law, C. K., *Proc. Combust. Inst.* 28:1917–1924 (2000).
2. Zeldovich, Ya. B., Barenblatt, G. I., Librovich, V. B., and Makhviladze, G. M., *The Mathematical Theory of Combustion and Explosions*, Consultants Bureau, New York, 1985.
3. Buckmaster, J. D., Joulin, G., and Ronney, P. D., *Combust. Flame* 84:411–422 (1991).
4. Ronney, P. D., *Combust. Flame* 82:1–14 (1990).
5. Ronney, P. D., Whaling, K. N., Abbud-Madrid, A., Gatto, J. L., and Pisowicz, V. L., *AIAA J.* 32(3):569–577 (1994).
6. Buckmaster, J. D., Smooke, M. D., and Giovangigli, V., *Combust. Flame* 94:113–124 (1993).
7. Wu, M. S., Ronney, P. D., Colantonio, R. O., and Vanzandt, D. M., *Combust. Flame* 116:387–397 (1999).
8. Lozinski, D., Buckmaster J. D., and Ronney, P. D., *Combust. Flame* 97:301–316 (1994).
9. Rogg, B., and Wang, W., *RUN-IDL: The Cambridge Universal Flamelet Computer Code, User Manual*, University of Cambridge, Cambridge, England, 1995.
10. Wu, M. S., Liu, J. B., and Ronney, P. D., *Proc. Combust. Inst.* 27:2543–2550 (1998).
11. Mueller, M. A., Kim, T. J., Yetter, R. A., and Dryer, F. L., *Int. J. Chem. Kinet.* 31:113–125 (1999).
12. Hubbard, G. L., and Tien, C. L., *J. Heat Transfer* 100:235–239 (1978).
13. Abid, M., Aung, K., VanZandt, D., Frate, D., and Ronney, P. D., "Effects of Lewis Number on Flame Ball Dynamics," AIAA 2001-0623, Thirty-Ninth Aerospace Sciences Meeting and Exhibit, AIAA, Reno, NV, January 8–11, 2001.
14. Law, C. K., and Egolfopoulos, F. N., *Proc. Combust. Inst.* 23:413–421 (1990).
15. Christiansen, E. W., Sung, C. J., and Law, C. K., *Combust. Flame* 124:35–49 (2001).
16. Frankel, M. L., and Sivashinsky, G. I., *Combust. Sci. Technol.* 31:131–138 (1983).
17. Buckmaster, J. D., Gessman, R., and Ronney, P. D., *Proc. Combust. Inst.* 24:53–59 (1992).
18. Gerlinger, W., Schneider, K., and Bockhorn, H., *Proc. Combust. Inst.* 28:793–799 (2000).